



Temperature Dependence of the Defect States in LWIR (100) and (111)B HgCdTe Epilayers for IR HOT Detectors

Krzysztof Murawski¹ · K. Majkowycz¹ · J. Sobieski² · M. Kopytko¹ · P. Martyniuk¹

Received: 13 February 2024 / Accepted: 30 May 2024 / Published online: 3 July 2024
© The Author(s) 2024

Abstract

HgCdTe epilayers grown by chemical vapor deposition (MOCVD) on GaAs substrates operating in the long-wave infrared range were characterized by the photoluminescence (PL) method. Photodiode and photoconductor designs, both (100) and (111)B crystallographic, were analyzed. Spectral current responsivity (R_p) and a PL signal approximated by a theoretical expression being the product of the density of states and the Fermi–Dirac distribution were used to determine the fundamental transition (energy gap, E_g). For all the samples, an additional deep-level-related transition associated with mercury vacancies (V_{Hg}) were observed. The energy distance of about 80 meV above the valence band edge was observed for all the samples. Moreover, measurements at low temperature showed shallow acceptor-level (As_{Te} and V_{Hg} as acceptors) transitions. In HgCdTe(100), due to the higher arsenic activation, As_{Te} was the dominant acceptor dopant, while, in HgCdTe(111)B, the main acceptor level was formed by the neutral V_{Hg} . The determined activation energies for As_{Te} and V_{Hg} dopants were of about 5 meV and 10 meV, respectively.

Keywords Defect states · HgCdTe · photoluminescence · infrared detectors

Introduction

The long-wave infrared (LWIR) range is extremely important for industrial and military applications.^{1–4} Currently, high-operating-temperature (HOT) infrared (IR) detectors are being widely developed and can operate at ambient temperature or be cooled using simple, cheap, and easy-to-use thermoelectric coolers. In this context, mercury cadmium telluride (MCT)-based devices continue to be widely used. However, market requirements are for constant development and the search for new solutions in this field. Current technology uses various growth techniques,^{5–8} crystallographic orientations,^{9–12} and different substrates. Detection devices operating in the LWIR range must meet rigorous standards. Therefore,

it is necessary to grow epitaxial layers with high crystallographic quality. Defects that occur in HgCdTe, such as mercury (V_{Hg}) and tellurium (V_{Te}) vacancies and tellurium antisites occupying mercury sites (Te_{Hg}), introduce shallow levels into the energy gap: V_{Hg} acts as an acceptor, while V_{Te} and Te_{Hg} act as donors. Furthermore, the use of arsenic as an acceptor dopant can result in the formation of As_{Te} (takes the place of Te). When As takes the place of the Hg site (under Te-rich growth conditions), it incorporates as a donor.^{13,14} Moreover, due to the existence of V_{Hg} , a possible acceptor-type $V_{\text{Hg}}\text{--As}_{\text{Hg}}$ complex can be formed. V_{Hg} defects can also be located deep in the band gap. Acting as generation–recombination centers, they influence the detection performance reducing the Shockley–Read–Hall carrier lifetime.

The analysis of defect states can be performed using various measurement techniques,^{15,16} e.g., band-to-band and shallow transitions can be determined by photoluminescence (PL). In special cases, deep defect transitions can also be detected.^{14,15,17} Therefore, the PL method is also useful for determining the position of the defect state in relation to the energy gap, as it is not entirely consistent in various studies. Some studies claim that the

✉ Krzysztof Murawski
krzysztof.murawski01@wat.edu.pl

¹ Institute of Applied Physics, Military University of Technology, 2 Kaliskiego St., 00-908 Warsaw, Poland

² VIGO Photonics S.A., 129/133 Poznańska Street, 05-850 Ożarów Mazowiecki, Poland

trap level in HgCdTe is at $0.5 E_g$ or $0.7 E_g$ and proportionally changes with temperature to E_g .¹⁸ However, there are studies claiming that the trap level does not change its position with temperature, but is fixed at a constant level in relation to the edge of the valence band (VB).^{9,15}

This paper shows the PL results for four samples with the *p*-type Hg_{1-x}Cd_xTe absorber. Photodiode and photoconductor designs, both (100) and (111)B crystallographic, have been measured. PL spectra were analyzed for the temperature range from 18 K to 300 K. To correctly determine the energy gap, the current responsivity (R_I) measurements and the theoretical relationship presented by Hansen were used.¹⁹ Furthermore, an analysis of the PL intensity on the excitation power was made.

Sample and Experimental Details

The (100) and (111)B HgCdTe epilayers were grown by an Aixtron AIX-200 MOCVD system on 2-inch (c.5 cm) (100) GaAs substrates. In each sample, the CdTe buffer layer was used in order to compensate the lattice mismatch between the HgCdTe epilayer and the GaAs substrate. The growth technique has been described in detail in Refs. 20, 21, and 22.

Figure 1a shows the design of both the (100) and (111)B $N^+/p/T/P^+/n^+$ photodiodes (marked as A and B, respectively). Both samples have a similar structure: the wide-bandgap N^+ contact layer, the *p*-type active layer, the wide-bandgap P^+ barrier, and an n^+ cap-contact layer. The transient layer (T) parameters are conditioned by interdiffusion processes during the MOCVD growth. The

assumed doping and Cd molar composition were similar in both samples, but the main difference was the absorber thickness. Figure 1b shows the design of a *p*-type photoconductor, also grown (100) and (111)B crystallographic (marked as a C and D, respectively). In this case, the main difference was also the absorber thickness.

For the PL measurements, all the structures were chemically etched by a Br:HBr diluted in deionized water solution (50:50:1 Br:HBr:H₂O) to a *p*-type absorber layer. The PL characteristics were measured using an FTIR Bruker Vertex 70v spectrometer in the step-scan mode,²³ a liquid-nitrogen-cooled MCT DS315 detector, and a lock-in amplifier (Fig. 2). The 640-nm line, mechanically chopped with a frequency of a 10 kHz laser, was used as an excitation. The PL spectra were collected in the temperature range from 300 to 18 K and excitation power from 200 to 10 mW. Due to the small molar composition used in the photoconductors, the energy gap at low temperatures was narrowed and the signal went beyond the system's measurement range; — the measurement was performed in a limited temperature range (from 140 to 300 K). All the characteristics were made in a vacuum.

The R_I measurements were performed using an FTIR-type Spectrum 2000 spectrophotometer, and a blackbody at a temperature of 1000 K. Photodiodes were bottom-illuminated, while the photoresistors were top-illuminated, as shown in Fig. 1. All the characteristics were measured for a bias of -0.2 V. The electrical area was 7.85×10^{-5} cm² for the photodiodes and 12.64×10^{-5} cm² for the photoconductors.

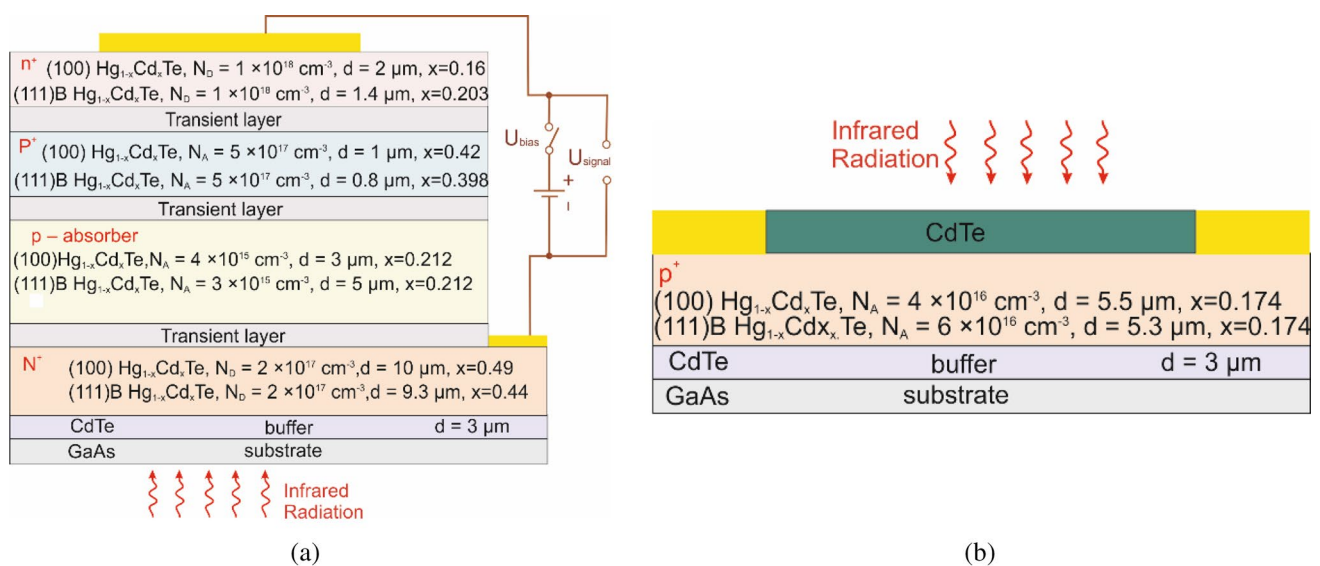


Fig. 1 Schematic of an LWIR HgCdTe $N^+/p/T/P^+/n^+$ photodiode (a), and a *p*-type photoconductor (b).

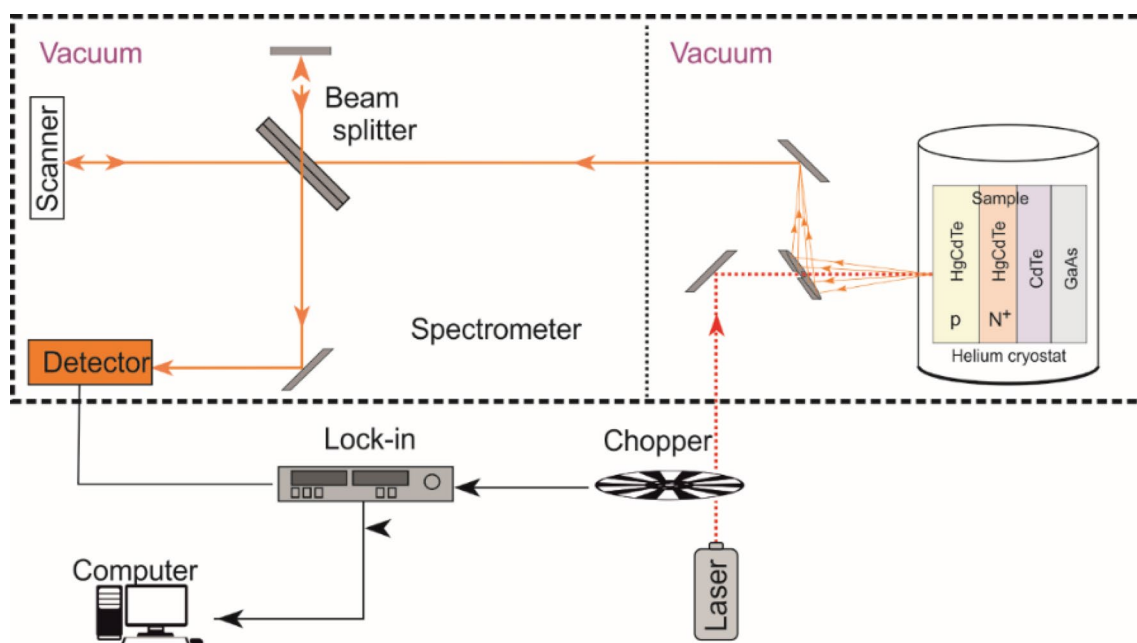


Fig. 2 PL measurement system.

Results and Discussion

The PL signals of the analyzed samples for high temperatures are shown in Fig. 3. At 300 K, the figure additionally shows the spectral current responsivity (R_I) as a second method to determine the E_g , which is the equivalent for the point where the detector response drops to 50% of the peak value.²⁴ The E_g based on the PL measurement was determined using a theoretical approximation which is proportional to the product of the joint density of states and the Fermi–Dirac distribution function.^{24,25} For A (Fig. 3a), the estimated E_g value is 195 meV at 300 K. An extra peak for the energy of 162 meV is also visible. As the temperature decreases, this transition disappears and another low-energy peak becomes visible for the energy of 86 meV. The same, most probably defect-related transition with an energy of 82 meV, is visible in B (Fig. 3b). Even though the assumed molar composition of the absorber of B was the same as that of A, the determined E_g has a smaller value of about 175 meV.

Both photoconductor samples (Fig. 3c and d), apart from the main energy transition with 130 meV for C and 128 meV for D at 300 K, have an apparent transition from the defect level with energies of 80 meV and 88 meV, respectively. An defect-related transition with an energy of 115 meV is visible in the PL spectrum of C. This transition disappears at lower temperatures.

Figure 4 shows the PL spectra measured for the photoconductors (sample A and B) at low temperatures. For sample A, three extra transitions can be seen, with the positions of 5 meV, 10 meV, and 18 meV below E_g , respectively. For sample B, only two extra transitions with energies of 4 meV and 8 meV below E_g can be seen.

Figure 5 shows the temperature dependence of all the visible optical transitions in the PL spectrum. Band-to-band transitions were fitted with theoretical Hansen's relationships. It can be seen that, for all the samples, the actual molar composition differs from that assumed in the growth process. The transition with the energy of about 80 meV is visible in all the analyzed samples. This is most likely a transition from the defect level to the VB. The constant with temperature transition energy indicates that the position of the defect level does not change with temperature, but is fixed at a constant distance from the edge of the VB. When temperature decreases and E_g becomes smaller than the defect level position, the defect-related PL peak disappears. This happens because the defect level enters the conduction band (CB), where it creates a so-called resonance state.^{15,26} Both samples with the (111)B orientation have one extra defect-related transition, with their temperature behavior analogous to that discussed above.

Moreover, below 80 K, extra transitions for the photoconductors become visible. Their distance from E_g is constant with temperature for all the transitions. The origin of all

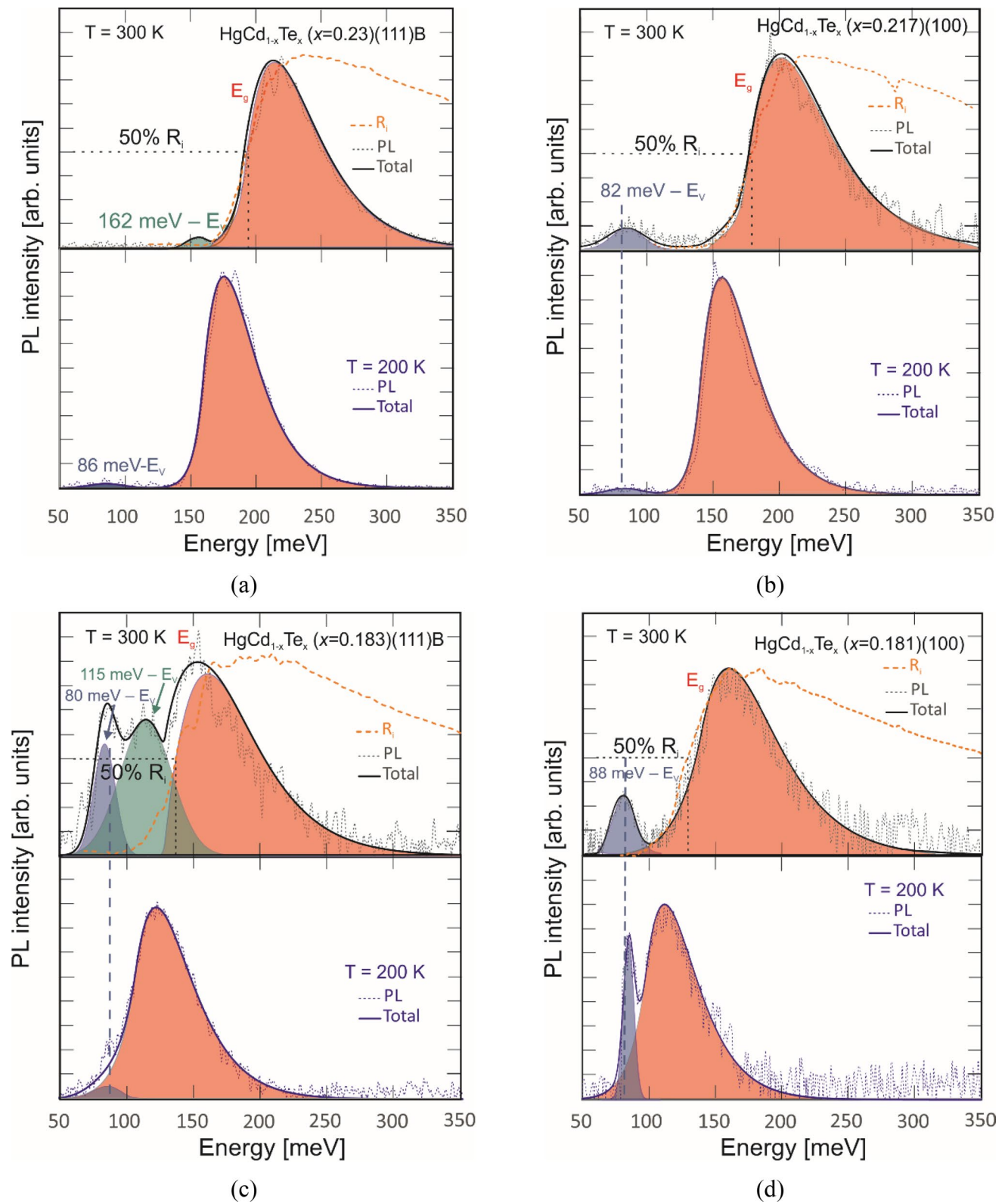


Fig. 3 PL and R_1 spectra measured at high temperatures for the LWIR HgCdTe A (a), B (b), C (c), and D (d).

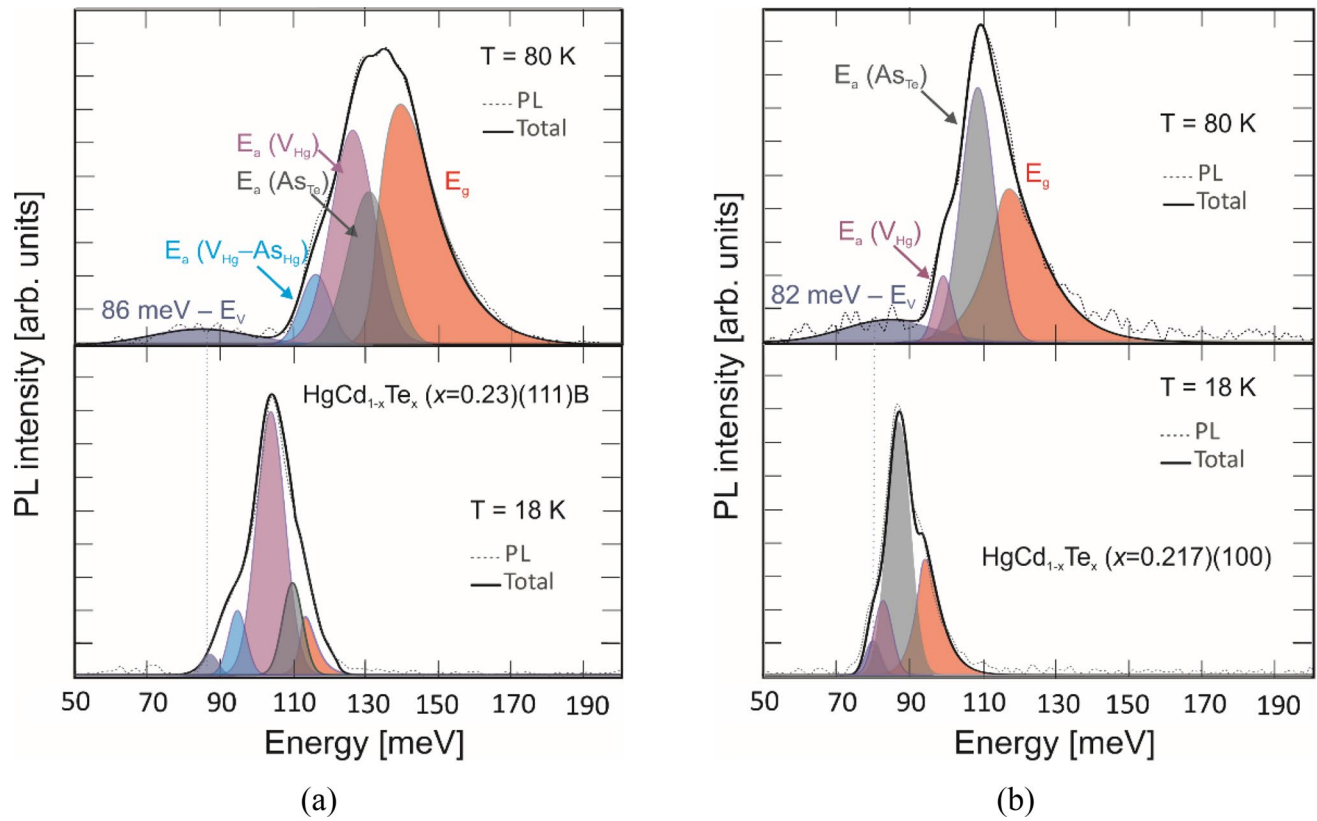


Fig. 4 PL spectra measured at low temperatures for the LWIR HgCdTe A (a), and B (b).

the PL peaks will be discussed further by analyzing the PL signal intensity as a function of the excitation laser power.

Figure 6 shows the analysis of the PL intensity dependence on the excitation power for photodiode-based structures at 18 K. Alpha (α) coefficients were determined based on the power law:

$$I_{PL} P \tag{1}$$

where I_{PL} is the PL peak intensity for a given excitation power P , and the exponent α indicates the transition type.²⁷ The extracted exponent factor $\alpha = 1$ corresponds to the band-to-band transitions, while $\alpha < 1$ corresponds to the shallow defect transitions, as well as deep defect transitions. The results for both samples are presented in Table I.

Deep defect levels with $\alpha = 0.75$ for sample A and $\alpha = 0.4$ for sample can be associated with mercury vacancies, which is confirmed by the literature data.²⁸ The distance of about 80 meV above the VB edge agrees with that determined by us in our previous work²⁹ of a defect level originating from the single negatively charged V_{Hg} :

$$E_T(V_{Hg}^{-1}) = 144x + 56 \tag{2}$$

where E_T is in [meV].

The extra peaks at temperatures below 80 K suggest a shallow acceptor transition. Two PL peaks with energies of ~ 5 meV and ~ 10 meV below the E_g can be assigned to the acceptor states of As_{Te} and V_{Hg} , respectively. Their activation energies coincide with the theoretical relationships given by^{28,30}:

$$E_{a1}(As_{Te}) = 42x + 1.36 - 1.4 \times 10^{-5} N_a^{1/3} \tag{3}$$

and

$$E_{a2}(V_{Hg}^0) = 91.1x - 6.93 \tag{4}$$

where E_{a1} and E_{a2} are in meV. The experimentally determined and calculated activation energies of the defect and acceptor levels are summarized in Table II.

As can be seen in Fig. 4, at 18 K, the dominant PL peak is related with the transition from the CB to the acceptor level, in A associated with V_{Hg} , while in B with As_{Te} . This may be due to the fact that the As incorporation in HgCdTe is higher in the (100) orientation than in the (111)B one.³¹ When As is not fully activated, it

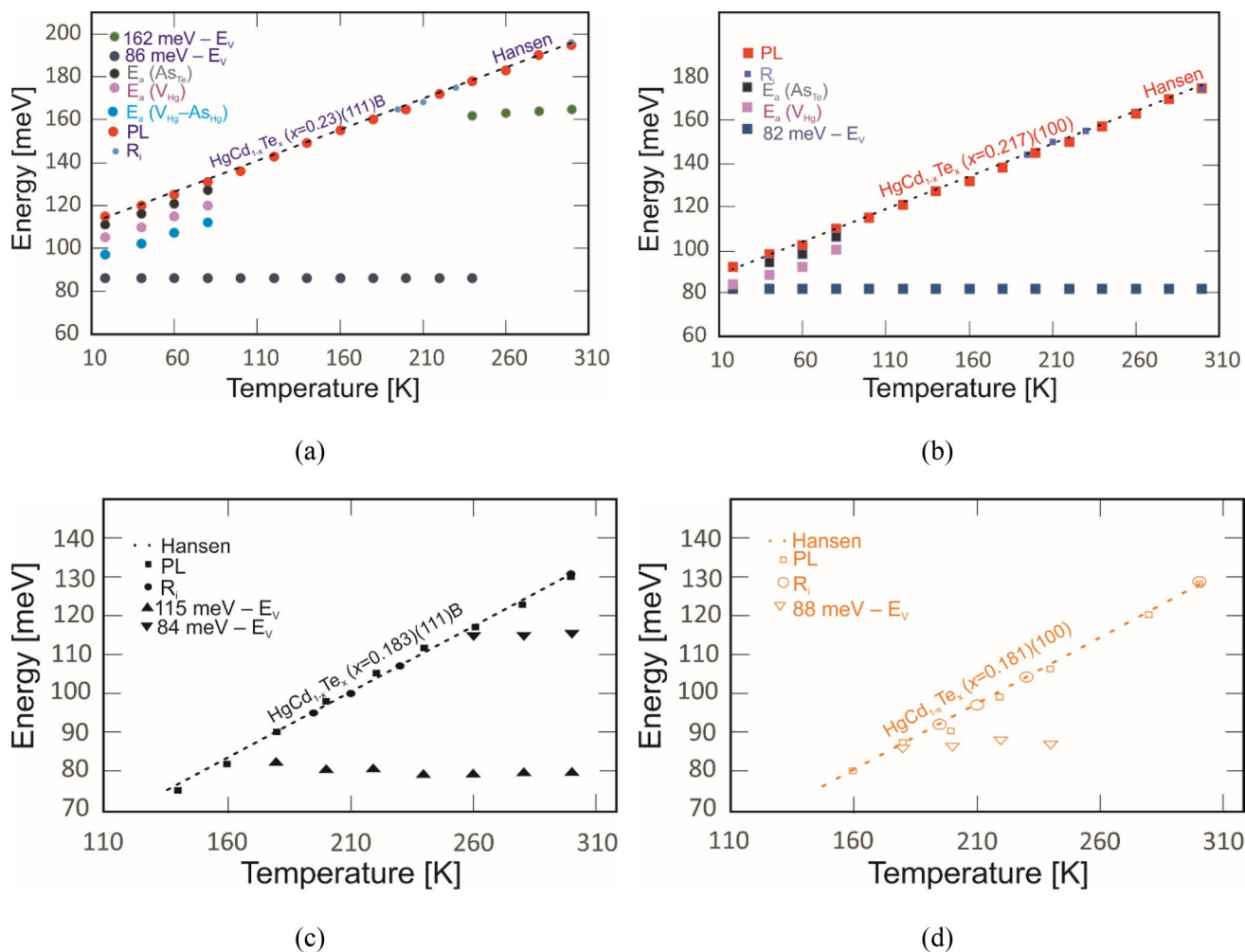


Fig. 5 Temperature dependence of the PL peaks energy for the LWIR HgCdTe A (a), B (b), C (c), and D (d). The E_g was determined from the PL and R_i measurements and compared to the Hansen relationship.

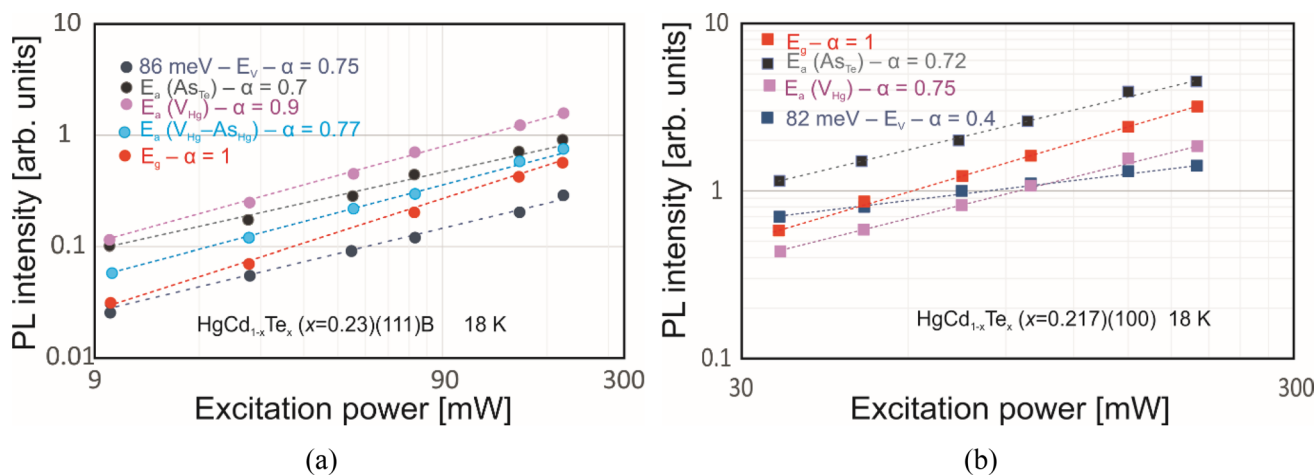


Fig. 6 PL intensity versus excitation power for the LWIR HgCdTe A (a), and B (b) at 18 K.

Table I The exponent factor α for the p -type HgCdTe at 18 K

Transition	Sample A ($x = 0.23$)	Sample B ($x = 0.17$)
	α	α
E_g	1	1
$E_{a1}(\text{As}_{\text{Te}})$	0.7	0.72
$E_{a2}(\text{V}_{\text{Hg}}^0)$	0.9	0.75
$E_{a3}(\text{V}_{\text{Hg}} - \text{As}_{\text{Hg}})$	0.77	–
$E_T(\text{V}_{\text{Hg}}^{-1})$	0.75	0.4

Table II Summary of the experimental and theoretical data for the p -type HgCdTe at 18 K

Sample	E_g [meV]		$E_T(\text{V}_{\text{Hg}}^{-1})$ [meV]		$E_{a1}(\text{As}_{\text{Te}})$ [meV]		$E_{a2}(\text{V}_{\text{Hg}}^0)$ [meV]	
	Exp.	Ref. 19	Exp.	Eq. 2	Exp.	Eq. 3	Exp.	Eq. 4
A ($x = 0.23$)	115	114.62	86	89.1	5	6.67	10	14
B ($x = 0.17$)	92	92.62	82	87.2	4	5.69	8	12.8

occupies the Hg site (As_{Hg}). Then, when the inactivated-As exists in sufficient density, V_{Hg} prefers to form the $\text{V}_{\text{Hg}}-\text{As}_{\text{Hg}}$ complex. Thus, the remaining PL peak in A with the energy of ~ 18 meV below the E_g can be assigned to the $\text{V}_{\text{Hg}}-\text{As}_{\text{Hg}}$ complex.

Conclusions

The results presented in this paper show PL measurements for p -type HgCdTe LWIR epilayers grown with photodiode and photoconductor designs on GaAs substrates. Two crystallographic orientations typical for HgCdTe were analyzed: (111)B and (100). The PL spectra temperature dependence shows band-to-band and extra defect- and dopant-related transitions. The deep level with the energy distance of ~ 80 meV above the VB edge is most likely associated with the single negatively charged V_{Hg} . It does not change its position with temperature. The measurements at cryogenic temperature show shallow acceptor levels associated with As_{Te} and V_{Hg} with the energies of ~ 5 meV and ~ 10 meV above the VB edge, respectively. In HgCdTe(100), due to higher arsenic activation, As_{Te} is the dominant acceptor dopant, while, in HgCdTe(111)B, the main acceptor level is formed by the neutral V_{Hg} . Moreover, due to the existence of an inactive acceptor dopant (As in the Hg sublattice), in HgCdTe(111)B there is a visible transition to the acceptor level created by the $\text{V}_{\text{Hg}}-\text{As}_{\text{Hg}}$ complex.

Funding This study was funded by the National Science Centre (Poland), grant no. UMO-2019/33/B/ST7/00614.

Conflict of interest The authors declare that they have no conflict of interest.

Open Access This article is licensed under a Creative Commons Attribution 4.0 International License, which permits use, sharing, adaptation, distribution and reproduction in any medium or format, as long as you give appropriate credit to the original author(s) and the source, provide a link to the Creative Commons licence, and indicate if changes were made. The images or other third party material in this article are included in the article's Creative Commons licence, unless indicated otherwise in a credit line to the material. If material is not included in the article's Creative Commons licence and your intended use is not permitted by statutory regulation or exceeds the permitted use, you will need to obtain permission directly from the copyright holder. To view a copy of this licence, visit <http://creativecommons.org/licenses/by/4.0/>.

References

- O. Gravrand, J. Rothman, P. Castelein, C. Cervera, N. Baier, C. Lobre, E. De Borniol, J.P. Zanatta, O. Boulade, V. Moreau, B. Fieque, and P. Chorier, Latest achievements on MCT IR detectors for space and science imaging. *Inf. Technol. Appl. XLII* 9819, 9819 (2016).
- H Lutz, R Breiter, D Eich, H Figgemeier, and S Hanna, "Towards high operating temperature and small pixel pitch MCT LWIR modules. In: Infrared Technology and Applications XLVIII. 12107. SPIE, (2022).
- P. Martyniuk, W. Gawron, P. Madejczyk, A. Rogalski, and J. Piotrowski, Modeling of HgCdTe LWIR detector for high operation temperature conditions. *Metrol. Meas. Syst.* 20(2), 159 (2013).
- I.W.A. Rogalski, Infrared detectors, Second Edition (2010).
- D. Eich, W. Schirmacher, S. Hanna, K.M. Mahlein, P. Fries, and H. Figgemeier, Progress of MCT detector technology at AIM towards smaller pitch and lower dark current. *J. Electron. Mater.* 46(9), 5448 (2017).

6. V.S. Varavin, I.V. Sabinina, GYu. Sidorov, D.V. Marin, V.G. Remesnik, A.V. Predein, S.A. Dvoretzky, V.V. Vasilyev, Yu.G. Sidorov, M.V. Yakushev, and A.V. Latyshev, Photodiodes based on p-on-n junctions formed in MBE-grown n-type MCT absorber layers for the spectral region 8 to 11 μm . *Infrared Phys. Technol.* 105, 103182 (2020).
7. N.K. Dhar, R. Dat, and A.K. Sood, Advances in infrared detector array technology. *Optoelectron. Adv. Mater. Dev.* (2013). <https://doi.org/10.5772/51665>.
8. A. Greenen, S. Bains, L. Hipwood, M. Lee, D. Owton, and K. McEwen, Further developments of 12 μm pixel dual waveband MWIR-LWIR infrared detectors using MOVPE grown MCT. In: *Infrared Technology and Applications XLVIII*. SPIE, 230–235 (2022).
9. X. Zhang, J. Shao, L. Chen, X. Lü, S. Guo, L. He, and J. Chu, Infrared photoluminescence of arsenic-doped HgCdTe in a wide temperature range of up to 290 K. *J. Appl. Phys.* 110(4), 043503 (2011).
10. A. Kębłowski, M. Kopytko, K. Młynarczyk, W. Gawron, J. Piotrowski, P. Martyniuk, and A. Rogalski, Investigation of hill-locks formation on (1 0 0) HgCdTe layers grown by MOCVD on GaAs epi-ready substrates. *Infrared Phys. Technol.* 84, 87 (2017).
11. M. Kopytko, J. Sobieski, W. Gawron, and P. Martyniuk, Study of HgCdTe (100) and HgCdTe (111) B heterostructures grown by MOCVD and their potential application to APDs operating in the IR range up to 8 μm . *Sensors* 22(3), 924 (2022).
12. T. Kryshchab, R.K. Savkina, A.B. Smirnov, M. Kladkevich, and V. Samoylov, Multi-band radiation detector based on HgCdTe heterostructure. *Phys. Status Solidi* 13(7–9), 639 (2016).
13. H. Duan, X. Chen, Y. Huang, and W. Lu, First-principles study of arsenic impurity clusters in molecular beam epitaxy (MBE) grown HgCdTe. *Solid State Commun.* 143(10), 471 (2007).
14. F.Y. Yue, S.Y. Ma, J. Hong, P.X. Yang, C.B. Jing, Y. Chen, and J.H. Chu, Optical characterization of defects in narrow-gap HgCdTe for infrared detector applications. *Chin. Phys. B* 28, 017104 (2019).
15. H. Jia-Yao, S. Lin, M. Shu-Fang, H. Bin, W. Guo-Dong, L. Qing-Ming, H. Xiao-Dong, S. Heng-Sheng, and X. Bing-She, Low temperature photoluminescence study of GaAs defect states. *Chin. Phys. B* 29(1), 010703 (2020).
16. L. Ciura, A. Kolek, A. Kębłowski, D. Stanaszek, A. Piotrowski, W. Gawron, and J. Piotrowski, Investigation of trap levels in HgCdTe IR detectors through low frequency noise spectroscopy. *Semicond. Sci. Technol.* 31(3), 035004 (2016).
17. K. Murawski, K. Majkowycz, M. Kopytko, and P. Martyniuk, Photoluminescence study of as doped p-type HgCdTe absorber for infrared detectors operating in the range up to 8 μm . *J. Electron. Mater.* 52(11), 7038 (2023).
18. D.L. Polla and C.E. Jones, Deep level studies of Hg_{1-x}Cd_xTe. *J. Appl. Phys.* 52, 5118 (1981).
19. G.L. Hansen, J.L. Schmit, and T.N. Casselman, Energy gap versus alloy composition and temperature in Hg_{1-x}Cd_xTe. *J. Appl. Phys.* 53(10), 7099 (1982).
20. P. Madejczyk, A. Kębłowski, W. Gawron, P. Martyniuk, M. Kopytko, D. Stepien, J. Rutkowski, J. Piotrowski, A. Piotrowski, and A. Rogalski, Uncooled middle wavelength infrared photoconductors based on (111) and (100) oriented HgCdTe. *Opt. Eng.* 56(9), 091602 (2017).
21. M. Kopytko, A. Kębłowski, P. Madejczyk, P. Martyniuk, J. Piotrowski, W. Gawron, K. Grodecki, K. Jóźwikowski, and J. Rutkowski, Optimization of a HOT LWIR HgCdTe photodiode for fast response and high detectivity in zero-bias operation mode. *J. Electron. Mater.* 46, 6045 (2017).
22. A. Piotrowski, P. Madejczyk, W. Gawron, K. Kłos, J. Pawluczuk, J. Rutkowski, J. Piotrowski, and A. Rogalski, Progress in MOCVD growth of HgCdTe heterostructures for uncooled infrared photo-detectors. *Infrared Phys. Technol.* 49(3), 173 (2007).
23. M. Motyka, G. Sęk, J. Misiewicz, A. Bauer, M. Dallner, S. Höfling, and A. Forche, Fourier transformed photoreflectance and photoluminescence of mid infrared GaSb-based type II quantum wells. *Appl. Phys. Express* 2(12), 126505 (2009).
24. K. Murawski, M. Kopytko, P. Madejczyk, K. Majkowycz, and P. Martyniuk, HgCdTe energy gap determination from photoluminescence and spectral response measurements. *Metrol. Meas. Syst.* (2023). <https://doi.org/10.24425/mms.2023.144395>.
25. M. Latkowska, R. Kudrawiec, F. Janiak, M. Motyka, J. Misiewicz, Q. Zhuang, A. Krier, and W. Walukiewicz, Temperature dependence of photoluminescence from InNAsSb layers: the role of localized and free carrier emission in determination of temperature dependence of energy gap. *Appl. Phys. Lett.* 102(12), 122109 (2013).
26. C.W. Myles, Charge state splittings of deep levels in Hg_{1-x}Cd_xTe. *J. Vac. Sci. Technol. A* 6(4), 2675 (1988).
27. T. Schmidt, K. Lischka, and W. Zulehner, Excitation-power dependence of the near-band-edge photoluminescence of semiconductors. *Phys. Rev. B* 45(16), 8989 (1992).
28. P. Capper and J. Garland, Mercury cadmium telluride growth, properties and applications. Wiley, United Kingdom (2011).
29. K. Majkowycz, K. Murawski, and M. Kopytko, New insight into defect energy levels in HgCdTe. *Infrared Physics & Technology*, to be published (2024).
30. X.H. Shi, S. Rujirawat, R. Ashokan, C.H. Grein, and S. Sivananthan, Ionization energy of acceptors in As-doped HgCdTe grown by molecular beam epitaxy. *Appl. Phys. Lett.* 73(5), 638 (1998).
31. P. Madejczyk, A. Piotrowski, W. Gawron, K. Kłos, J. Pawluczuk, J. Rutkowski, J. Piotrowski, and A. Rogalski, Growth and properties of MOCVD HgCdTe epilayers on GaAs substrates. *Opto-Electron. Rev.* 13(3), 239 (2005).

Publisher's Note Springer Nature remains neutral with regard to jurisdictional claims in published maps and institutional affiliations.